

# Triangular Patch Yagi Antenna with Reconfigurable Pattern Characteristics

Jian Zhang, Xue-Song Yang, Jia-Lin Li, and Bing-Zhong Wang

Institute of Applied Physics,  
University of Electronic Science and Technology of China, Chengdu, 610054, China  
zhjian0928@163.com, xsyang@uestc.edu.cn, jialinuestc@gmail.com, bzwang@uestc.edu.cn

**Abstract** — A pattern reconfigurable Yagi patch antenna is proposed. The antenna is composed of three triangular microstrip patches, i.e., one driven patch and two parasitic patches. By controlling switches, which are installed on the parasitic patches, the radiation pattern of the antenna can point to three different directions, covering an elevation range from  $-61^\circ$  to  $+63^\circ$  in the E-plane. The simulated and measured results are presented and they agree with each other in reasonable precision.

**Index Terms** — Microstrip antennas, pattern reconfigurable antennas, Yagi-Uda arrays.

## I. INTRODUCTION

Reconfigurable antennas have received a lot of attention since they can provide various functions in operating frequency, beam pattern, and polarization, etc. [1-2]. The antenna that can change radiation pattern and maintain operating frequency is called pattern reconfigurable antenna. The pattern reconfigurable antenna has the potential to improve the overall system performance by changing beam directions to avoid electronic jamming or noise source, improve security and save energy [3-4].

It is in great demand for pattern reconfigurable antennas in the fields of wireless communications, satellite communications, radars, etc. Usually, phased antenna arrays are used to accomplish beam steering [5-6]. In the traditional microstrip phased array, where the array elements have fixed beam patterns, the beam scanning is accomplished by using phase shifters. As a result, the scanning range of the array is somewhat limited [6]. If the

array element is replaced by the pattern reconfigurable antenna, an additional degree of freedom is provided and the scanning range of the array can be enlarged correspondingly [7-8]. Furthermore, the pattern reconfigurable antenna has found application in MIMO wireless communications to improve the communication system performance [9].

Yagi-Uda antenna has the ability to tilt broadside pattern to endfire pattern. Based on the principle of Yagi-Uda antenna, some pattern reconfigurable antennas have been reported [2, 10-12]. For example, a pattern reconfigurable Yagi microstrip dipole antenna has been presented [10]. By adjusting the lengths of parasitic dipoles, the main beams can change directions in the H-plane. Another reconfigurable Yagi antenna is proposed in [11]. All the elements are square patches and have switches installed in the slots on parasitic patches. By changing the states of switches, the parasitic elements can be used as directors or reflectors. The main beams of three modes of this antenna can cover a continuous range in the E-plane in the upper half space.

Most of the reported reconfigurable antennas use switches to achieve antennas reconfigurability [13-16]. With the rapid development of MEMS, semiconductor, and photoconductor technologies, most of the reconfigurable antennas can be easily fabricated using different switches. PIN diode has been extensively explored for designing various reconfigurable antennas due to a lot of advantages, such as good reliability, compact size, high switching speed, and small resistance and capacitance in the ON and OFF states. Although the PIN diode enables fast configuration speed, it is lossy and can affect the antenna performance if

not properly designed. An alternative is RF MEMS switch, which has excellent properties, such as low loss, low power consumption and high isolation. Photoconductor switch has an outstanding characteristic of immunity to electromagnetic waves, consequently, without interference to antenna radiation pattern. The main disadvantage of MEMS and photoconductor switches is the high cost.

Some papers have compared the effects of the actual switches and the ideal switches [15-16]. In [16], a PIN diode was used to configure the operating frequency of a slot antenna. By controlling its biasing voltage, a diode can be easily turned ON and OFF. It is always very desirable to have a diode that has low loading effect (OFF state) and small resistance (ON state). Obviously, the ON-state resistance can result in power dissipation and degrade the antenna radiation efficiency. For such a reconfigurable antenna, the total dissipated power depends on the diode's ON resistance and the number of switches being used.

A novel triangular patch Yagi antenna, consists of three triangular patches, is proposed in this paper. By controlling the switches installed on the parasitic patches, the antenna can work at three modes, and the maximum beam direction shifts among  $-32^\circ$ ,  $+10^\circ$  and  $+34^\circ$  as predicted, where '+' indicates that the radiation pattern tilts towards the positive  $x$ -axis and '-' towards the negative  $x$ -axis. The state of the director is different from that in [11], i.e. the director in the proposed antenna has a similar state to the reflector in [11]. Besides, the proposed antenna has only two parasitic elements, which makes the antenna much smaller than that in [11], which makes the antenna more easily be used in antenna arrays. Furthermore, the loaded slots are simpler, and only four switches are needed to control the radiation pattern direction, which reduces the cost and makes the antenna mode adjusting more convenient.

## II. ANTENNA DESIGN

The principle of Yagi-Uda patch antenna with a driven and three parasitic rectangular patch elements is well known [12]. In this initiative article, the sizes of parasitic patches are different, with the small patches used as directors and the largest one acted as a reflector. In this paper, the proposed triangular patch Yagi antenna has three

elements, one driven patch and two parasitic patches, as shown in Fig. 1. All elements are equilateral triangular patches, and are supported on the top side of a grounded substrate with height of 0.76 mm and dielectric constant of 2.94. The parasitic elements are two identical triangular patches and a little smaller than the driven one. A coaxial probe is used to feed the antenna from the bottom of the substrate and the feed point is located at the symmetry axis of the antenna. There is a narrow rectangular slot on each parasitic patch, and two switches are installed in each slot to change the equivalent capacitance and inductance of the patch. Figure 2 (a) shows the detail of the parasitic element.

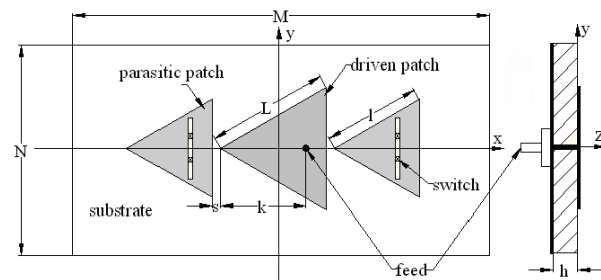


Fig. 1. Geometry of the proposed antenna.

The parameters of the antenna are as follows:  $M=34$  mm,  $N=17$  mm,  $a=0.4$  mm,  $b=1.4$  mm,  $c=0.4$  mm,  $d=5.0$  mm,  $m=5.0$  mm,  $k=7.0$  mm,  $L=10.0$  mm,  $l=8.0$  mm,  $s=0.7$  mm and  $h=0.76$  mm.

By controlling the switches on the patch, two states of the parasitic element can be obtained. When both switches on the parasitic patch are open, i.e., the switches are "OFF", the parasite is acted as a director, and this state is called "D", as shown in Fig. 2 (b). This is different from the antenna in [11], where when all the switches on the parasitic patch are open, the parasite is acted as a reflector. Meanwhile, when both switches are closed, the state of the parasite is called "N", as shown in Fig. 2 (b), and the patch has nearly no effect on the radiation pattern, which is similar to that in [11]. By combining the states of parasitic elements at two sides of the driven patch, at least three different modes of the antenna, i.e., DN, ND and NN, can be obtained. DN means that the parasitic element at the left side acts as a director and the right side one has no effect on the pattern. With reference to the coordinate in Fig. 1, the main beam tilts to the negative  $x$ -axis. Likewise,

ND indicates that the right side parasitic acts as a director and the radiated beam directs to the positive  $x$ -axis. NN means both sides of parasites have nearly no effect on the radiation pattern, and then the antenna has a broadside pattern. By adjusting modes of the antenna, the radiation pattern is reconfigured.

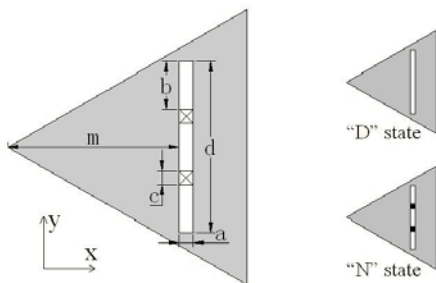


Fig. 2. (a) Geometry of the parasitic patch. (b) the specific structures at two states, where the black squares stand for the closed switches.

### III. SIMULATED AND MEASURED RESULTS

#### A. Ideal Switches

Ansoft's HFSS is used to simulate the performance of the antenna. To validate the simulation, two prototypes, which are at modes DN and ND, respectively, are fabricated and measured. Metallic pads take the places of closed switches in the simulation and fabrication. Figure 3 shows one fabricated model at mode DN.



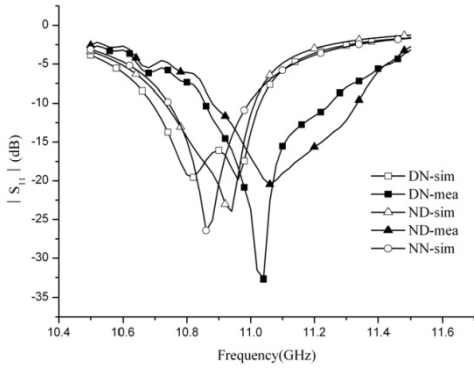
Fig. 3. Fabricated antenna model (mode DN).

The simulated and measured  $|S_{11}|$  are shown in Fig. 4. From the simulation results, it can be seen that the resonant frequencies of all three modes are around 10.9 GHz, and the common bandwidth is from 10.74 GHz to 11.0 GHz, about 260 MHz. Compared with the simulated results, the measured resonant frequencies shift upward by about 0.15 GHz, with the common bandwidth from 10.88 GHz to 11.25 GHz. In addition, for the simulation results, a bulge appears between 10.8~11.0GHz in

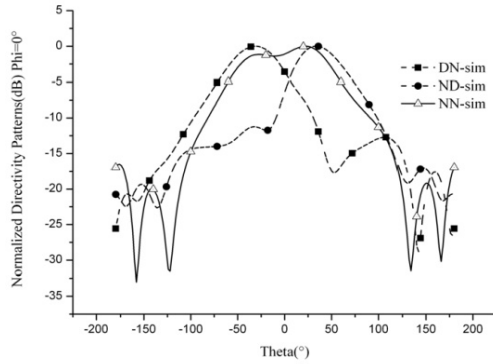
the DN mode, means that the resonant frequencies of the driven patch and the parasitic patches at this mode are not very closed to each other, where the lower resonance is from the driven patch and the upper one is from the D state parasitic patch [11, 15]. If the slot on the parasitic patch is longer, the upper resonance frequency will decrease, and more closed to the lower one. Consequently, the bulge will disappear. For the other modes, the resonant frequencies of different patches are much closed to each other and then seem to be one resonance. However, appropriate separate of the resonant frequencies of different patches is benefit to the widening of the bandwidth. Preliminary analysis shows that the deviation of resonant frequency of measurement from simulation should be caused by the inaccuracy of dielectric constant and the inevitable machining error.

The simulated maximum beams direct to the elevation angles of  $-32^\circ$ ,  $+10^\circ$  and  $+34^\circ$ , when the antenna works at modes DN, NN and ND, respectively, as shown in Fig. 4(b). At modes DN, NN and ND, the 3-dB beamwidths in the E-plane are from  $-61^\circ$  to  $-3^\circ$ , from  $-45^\circ$  to  $+50^\circ$  and from  $+10^\circ$  to  $+63^\circ$ , respectively. That means the radiation pattern of the antenna can cover the elevation range from  $-61^\circ$  to  $+63^\circ$  in the upper half space by switching among these three modes. Compared with the antenna in [11], whose scanning angle is from  $-69^\circ$  to  $+67^\circ$ , the beam coverage of the proposed antenna is a little narrower, but its whole dimensions are much smaller. The simulated antenna gains, corresponding to the operating frequency of 10.9 GHz, are 8.44, 6.80 and 8.85 dBi at modes DN, NN and ND, respectively.

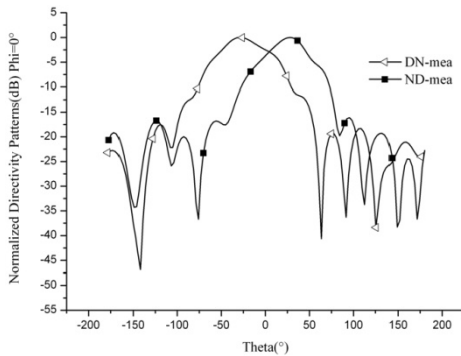
Figure 5 shows the current distribution at the modes DN, ND and NN, respectively. When the switches on the left side parasitic patch are open, strong current distribution arises around the slot and also the driven patch bevel edges close to the parasite. While the switches on the right side parasitic patch are open, strong current distribution arises around the slot, but on the driven patch, only weak current appears at the driven patch bevel edges. However, when all the switches are closed, strong current distribution appears at the driven patch, including the bevel edges and the central part. Therefore, both the slots and the shape of the patches have Fig. 5 shows the current distribution.



(a)

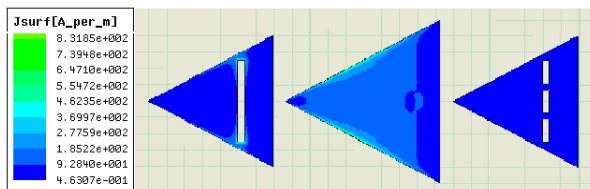


(b)

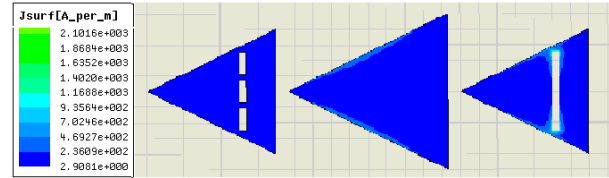


(c)

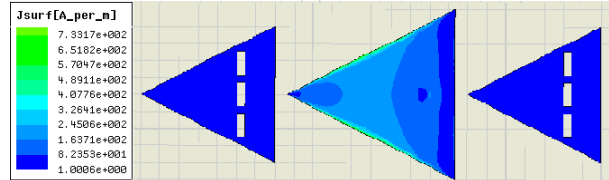
Fig. 4. S parameters and radiation patterns of three modes. (a) Simulated and measured S parameters. (b) Simulated radiation patterns in the E-plane (xoz-plane). (c) Measured radiation patterns in the E-plane (xoz-plane).



(a)



(b)



(c)

Fig. 5. current distribution at different modes. (a) Mode DN. (b) Mode ND. (c) Mode NN.

To validate the simulated results, the radiation patterns of modes DN and ND are measured as well. The measured radiation patterns are shown in Fig. 4(c). From the figure, it can be seen that the measured data coincide well with the simulated ones. The detailed data of the radiation patterns are listed in Table 1.

Table 1: Data of simulation and measurement

M	CI	BW(GHz)	MD	HPBW
DN	Sim	10.69-11.03	-32°	-61°~ -3°
	Mea	10.85-11.25	-30°	-53°~ 4°
ND	Sim	10.75-11.01	34°	10°~ 63°
	Mea	10.88-11.33	29°	5°~ 50°

In Table 1, M means the modes, CI means the Classification, BW is the bandwidth, MD is maximal direction in elevation, and HPBW is the half power beamwidth in elevation.

### B. RF MEMS Switches

HFSS simulations on simplified models of RF MEMS switches integrated into reconfigurable patch antennas have been implemented to examine the switches effects on the antennas [13-15]. The simulation and measurement results indicate that the RF MEMS switches have limited effect on the resonant frequency and radiation pattern. Furthermore, by modifying the antenna structure, such as the slot dimension, the reactance effect introduced by the RF MEMS switches can be eliminated [15].

The structures of a RF MEMS switch model at “ON” and “OFF” states are shown in Fig. 6. The

model consists of a microstrip line and a switch base without the metal ground. The dimensions of switch base are  $1.0 \text{ mm} \times 1.0 \text{ mm} \times 0.25 \text{ mm}$ , and are composed of silicon substrate ( $\epsilon_r=11.9$ ). The width ( $W$ ) of the microstrip line is  $0.05 \text{ mm}$ , and there is a gap ( $S=0.05 \text{ mm}$ ) when the switch is at ‘OFF’ state (Fig. 6 (a)).

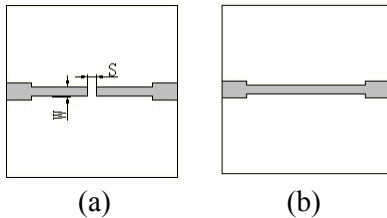


Fig. 6. Simulation model of a RF MEMS switch. (a) ‘OFF’ state. (b) ‘ON’ state.

In order to investigate the effect of the switch size on the antenna, another MEMS model with size of  $0.4 \text{ mm} \times 0.4 \text{ mm} \times 0.25 \text{ mm}$  is used in the simulation. In addition, the length of the slot ( $d=5 \text{ mm}$ ) will be modified to fit two different sizes of switch models. When the large size model ( $1.0 \text{ mm} \times 1.0 \text{ mm} \times 0.25 \text{ mm}$ ) is used,  $d$  is set to  $4.5 \text{ mm}$ . When the small size model ( $0.4 \text{ mm} \times 0.4 \text{ mm} \times 0.25 \text{ mm}$ ) is used,  $d$  is  $4.8 \text{ mm}$ .

Figure 7 shows the  $|S_{11}|$  and beam radiation patterns at mode DN when two different sizes of switch models are used. Switch 1 stands for the size of MEMS model of  $1.0 \text{ mm} \times 1.0 \text{ mm} \times 0.25 \text{ mm}$ , and Switch 2 is that of  $0.4 \text{ mm} \times 0.4 \text{ mm} \times 0.25 \text{ mm}$ . Compared with the simulated results of two different size switches, both S parameters and radiation patterns at mode DN coincide well with each other. Therefore, it can prove that the difference in size of RF MEMS switches has very little effect on the resonance frequency and beam patterns.

**C. PIN diode switches**

The PIN diode switches are also applied into the reconfigurable antennas, and some analytic methods are given in [16]. A PIN diode can be treated as an equivalent circuit shown in Fig. 8. In the HFSS simulation, the ‘RLC’ boundary patch often stands for a PIN diode switch model. When the PIN diode is at ‘ON’ state, it can be regarded as a small equivalent resistance, and when at ‘OFF’ state, it can be regarded as a small capacitance. By adjusting the PIN-diode equivalent capacitance on the antenna, the

radiation pattern is changed. The radiation patterns of mode DN with different PIN diode capacitance are shown in Fig. 9. With the increase of capacitance, the side lobe level increases correspondingly. Therefore, the capacitance should be as small as possible.

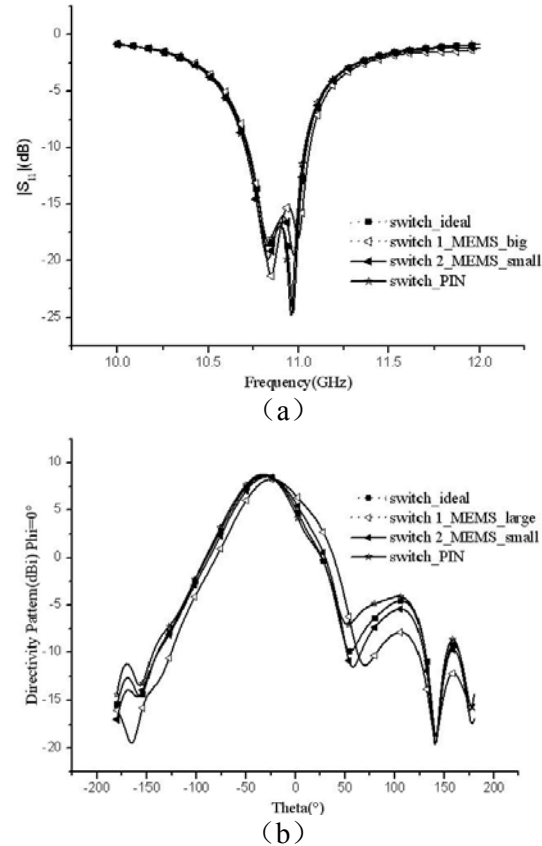


Fig. 7. S parameters and radiation patterns of ideal, MEMS and PIN switches. (a) S parameters. (b) Radiation patterns.

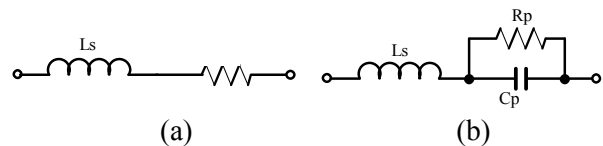


Fig. 8. The equivalent circuit of the PIN diode switch. (a) ‘ON’ state. (b) ‘OFF’ state.

The MPP4203 PIN-diode has an equivalent capacitance of  $0.08 \text{ pF}$ , and the other parameters can be found in [16]. The performance of the antenna with this PIN diode used is investigated by simulation. The S parameter and radiation pattern at Mode DN are shown in Fig. 6 as well. Here, the slot length  $d$  is shortened from  $5 \text{ mm}$  to  $4.8 \text{ mm}$ .

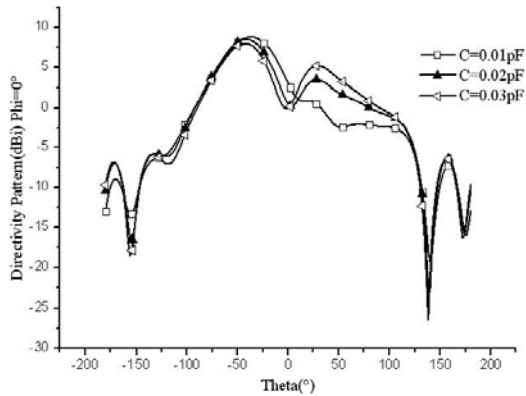


Fig. 9. Radiation patterns at mode DN with different equivalent capacitances of PIN diode switches.

It can be seen that for the results of the two RF MEMS switch models, PIN diode switch model and ideal switch model coincide very well with each other, except the modification of the slots on the parasitic patches.

However, in this simulation, the bias control circuit of the actual switches is not taken into account. For the actual switches, in order to minimize the effect of bias control circuit on the antenna, some methods must be adopted. The key is to isolate the RF signal from the DC control circuit. For example, for PIN diode switch, a low-pass filter structure can be inserted between the bias supply and the antenna. An inductive choke, which is in series with the bias line, and an RF-bypass capacitor, which is in parallel with the RF power supply output impedance, can be used to provide good RF/DC isolation [17]. Of course, with the bias control circuit installed, the impedance matching of the antenna must be tuned once again.

#### IV. CONCLUSION

In this paper, a novel triangular patch Yagi-Uda antenna with reconfigurable pattern characteristics is reported. Three modes of the antenna can be obtained by adjusting switches installed on the parasitic patches. The antenna can change the beam pattern and maintain the operating frequency. Pattern coverage from  $-61^\circ$  to  $63^\circ$  in the E-plane in the upper half space has been shown by simulation, and the measurement results have validated the simulation ones. Compared with that reported in [11], this antenna has fewer

parasitic elements, simpler structure and similar radiation beam coverage.

In the simulation, RF MEMS switches and PIN diode switches are integrated with the antenna. The simulated results show that very similar performances of the antenna can be obtained with different switches. The antenna can be used in mobile communications, satellite communications and radars, such as on aircrafts, ships and vehicle-mounted devices. In the near future, further investigation will be performed when actual switches are installed on the antenna.

#### ACKNOWLEDGMENT

This work was supported by the Fundamental Research Funds for the Central Universities (ZYGX2009J039) and the Natural Science Foundation of China (61271027).

#### REFERENCES

- [1] B.-Z. Wang, S. Xiao, and J. Wang, "Reconfigurable Patch-antenna Design for Wideband Wireless Communication Systems," *IET Microwaves, Antennas and Propagation*, vol. 1, no. 2, pp. 414-419, April, 2007.
- [2] H. A. Majid, M. K. A. Rahim, M. R. Hamid and M. F. Ismail, "Frequency and Pattern Reconfigurable Yagi Antenna," *Journal of Electromagnetic Waves and Applications*, vol. 26, no. 2-3, pp. 379-389, 2012.
- [3] W. S. Kang, J. A. Park and Y. J. Yoon, "Simple Reconfigurable Antenna with Radiation Pattern," *Electronics Letters*, vol. 44, no. 3, pp. 182-183, Jan. 2008.
- [4] Y. Yusuf and X. Gong, "A Low-cost Patch Antenna Phased Array with Analog Beam Steering using Mutual Coupling and Reactive Loading," *IEEE Antennas and Wireless Propagation Letters*, vol. 6, pp. 169-171, 2007.
- [5] M. R. Islam and M. Ali, "Elevation Plane Beam Scanning of a Novel Parasitic Array Radiator Antenna for 1900 MHz Mobile Handheld Terminals," *IEEE Transactions on Antennas and Propagation*, vol. 58, no. 10, pp. 3344-3352, Oct. 2010.
- [6] Z. J. Zhang, L. Jin and X. R. Shu, "Radar Antenna Technology," Publishing House of Electronics Industry, Beijing, 2007 (in Chinese).
- [7] S. Xiao, Y. Y. Bai, B. Z. Wang and S. Gao, "Scan Angle Extension by Array with Pattern Reconfigurable Elements," *Applied Computational Electromagnetics Society (ACES) Journal*, vol. 24, pp. 453-457, 2009.

- [8] Y. Y. Bai, S. Xiao, B. W. Wang and S. Gao, "Two-Dimensional Pattern Scanning by Linear Phased Array with Pattern Reconfigurable Elements," *Applied Computational Electromagnetics Society (ACES) Journal*, vol. 25, no. 2, pp. 144-148, February 2010.
- [9] C. P. Sukumar, H. Eslami, A. M. Eltawil and B. A. Cetiner, "Link Performance Improvement using Reconfigurable Multiantenna Systems," *IEEE Antennas and Wireless Propagation Letters*, vol. 8, pp. 873-876, 2009.
- [10] S. Zhang, G. H. Huff, J. Feng, and J. T. Bernhard, "A Pattern Reconfigurable Microstrip Parasitic Array," *IEEE Transactions on Antennas and Propagation*, vol. 52, no. 10, pp. 2273-2776, Oct. 2004.
- [11] X.-S. Yang, B.-Z. Wang, W. Wu, and S. Xiao, "Yagi Patch Antenna with Dual-band and Pattern Reconfigurable Characteristics," *IEEE Antennas and Wireless Propagation Letters*, vol. 6, pp. 169-171, 2007.
- [12] J. Huang and A. C. Densmore, "Microstrip Yagi Array Antenna for Mobile Satellite Vehicle Application," *IEEE Transactions on Antennas and Propagation*, vol. 29, pp. 1024-1030, July 1991.
- [13] G. H. Huff and J. T. Bernhard, "Integration of Packaged RF MEMS Switches with Radiation Pattern Reconfigurable Square Spiral Microstrip Antennas," *IEEE Transactions on Antennas and Propagation*, vol. 54, no. 2, pp. 464-469, Feb. 2006.
- [14] H. Rajagopalan, Y. Rahmat-Samii, and W. A. Imbriale, "RF MEMS Actuated Reconfigurable Reflectarray Patch-slot Element," *IEEE Transactions on Antennas and Propagation*, vol. 56, no. 12, pp. 3689-3699, Dec. 2008.
- [15] X.-S. Yang, B.-Z. Wang, S. H. Yeung, Q. Xue, and K. F. Man, "Circularly Polarized Reconfigurable Crossing Yagi Patch Antenna," *IEEE Antennas and Propagation Magazine*, vol. 53, no. 5, pp. 65-80, 2011.
- [16] J. H. Lim, G. T. Back, Y. I. Ko, C. W. Song, and T. Y. Yun, "A Reconfigurable PIFA using a Switchable PIN-diode and a Fine-tuning Varactor for USPCS/WCDMA/m-WIMAX/WLAN," *IEEE Transactions on Antennas and Propagation*, vol. 58, no. 7, pp. 2404-2411, July 2010.
- [17] Microsemi-Watertown, "The PIN Diode Circuit Designers' Handbook," pp. 7, 1992.



**Jian Zhang** received the B. Sc. degree in Electronic Information Science and Technology from UESTC, Chengdu, China, in 2009. He is currently working toward the M. Sc. Degree in UESTC. His current research interests include reconfigurable antennas and arrays.



**Xue-Song Yang** received the B. Eng. degree in Applied Electronic Technology from Huazhong University of Science and Technology (HUST), Wuhan, China, and the Ph.D. degree in Radio Physics from UESTC, Chengdu, China.

She joined the UESTC in 2002, where she is currently an associate professor. From Jan. 2007 to July 2008, she was a senior research associate and then a research fellow at the City University of Hong Kong. From Dec. 2009 to Dec. 2010, she was a Visiting Scholar at the University of Southern California, USA. Her current research interests include reconfigurable antennas, UWB antennas, MIMO antennas, and wireless communications channel modeling.



**Jia-Lin Li** received the M. Sc. degree from UESTC, Chengdu, China, in 2004, and the Ph. D. degree from the City University of Hong Kong, Hong Kong, in 2009, both in electronic engineering. Since Sept. 2009, he has been with the Institute of Applied Physics, School

of Physical Electronics, UESTC, where he is currently a Professor. His research interests include the high performance active/passive microwave/millimeter-wave antennas, circuits and systems realized on PCB, multilayer PCB, LTCC, etc.



**Bing-Zhong Wang** received the Ph.D. degree in electrical engineering from UESTC, Chengdu, China, in 1988.

He joined the UESTC in 1984 and is currently a Professor there. He has been a Visiting Scholar at the University of Wisconsin-Milwaukee, a Research Fellow at the City University of Hong Kong, and a Visiting Professor in the Electromagnetic Communication Laboratory, Pennsylvania State University. His current research interests are in the areas of computational electromagnetics, antenna theory, and computer-aided design for microwave circuits.